Applied Catalysis B: Environmental 111–112 (2012) 509–514

Contents lists available at SciVerse ScienceDirect

Applied Catalysis B: Environmental

journal homepage: www.elsevier.com/locate/apcatb

Quantitative determination of average rhodium oxidation state by a simple XANES analysis

Ken-ichi Shimizu[a,*], Tomonori Oda[b], Yoshinori Sakamoto[c], Yuichi Kamiya[c], Hisao Yoshida[d], Atsushi Satsuma[b]

[a] Catalysis Research Center, Hokkaido University, N-21, W-10, Sapporo 001-0021, Japan
[b] Department of Molecular Design and Engineering, Graduate School of Engineering, Nagoya University, Nagoya 464-8603, Japan
[c] Research Faculty of Environmental Earth Science, Hokkaido University, Kita 10 Nishi 5, Sapporo 060-0810, Japan
[d] Department of Applied Chemistry, Graduate School of Engineering, Nagoya University, Furo-cho, Chikusa-ku, Nagoya 464-8603, Japan

ARTICLE INFO

Article history:
Received 14 October 2011
Received in revised form 27 October 2011
Accepted 1 November 2011
Available online 7 November 2011

Keywords:
XANES
Rhodium
Characterization
Oxidation state
Heterogeneous catalysis

ABSTRACT

Quantitative determination of average rhodium oxidation state for supported rhodium catalyst was examined by using Rh L_3-edge XANES (X-ray absorption near-edge structure) spectra. A series of Rh-loaded SiO_2 catalysts (Rh_2O_x/SiO_2) containing different amount of Rh metal and Rh_2O_3 phases were prepared, and the average oxidation number (x) was determined by the amount of CO_2 formed during CO reduction treatment as the final step of catalyst preparation. L_3-edge XANES spectra of these samples were recorded, and the white line area intensity of the spectra was evaluated. A good linear relationship was confirmed between the white line area intensity and the average oxidation number (x), indicating that the oxidation state of Rh species in structurally unknown Rh samples could be quantitatively determined by a simple L_3-edge XANES analysis. The effect of the oxidation number (x) on the Rh_2O_x/SiO_2-catalysed CO oxidation was discussed, in order to demonstrate a utility of this method in a catalytic study.

1. Introduction

Platinum-group-metals (PGMs), especially Pt, Pd, and Rh, have been indispensable elements in various industrial catalyses including automotive three-way catalysis. The rational design of the new PGM catalysts requires fundamental knowledge of the correlation between structure (size, shape, and oxidation state) and catalytic activity. It is known that the oxidation state strongly affect the catalytic activity of supported Pt [1–10], Pd [11–13], and Rh [14–18] catalysts for various reactions such as hydrogenation and oxidation. The effect of Pt oxidation state on the catalytic activity has been most extensively studied. Generally, Pt in metallic state shows higher catalytic performance than that in oxidized state. However, a few reports showed that partially oxidized Pt exhibited higher activity than the metallic one [7]. For supported Pd catalysts, Yazawa et al. [11,12] studied the relation between the Pd oxidation state and their catalytic activity for propane combustion and concluded that partially oxidized Pd was effective. It is well known that aging of Rh/Al_2O_3 catalyst in an oxidizing environment at high temperature causes the oxidation of the rhodium, which results in catalyst deactivation [15–17]. In contrast, Somorjai and co-workers [18] recently demonstrated that the active phase of Rh catalysts for CO oxidation was a surface oxide layer over the metal nanoparticles. These examples demonstrate that the oxidation state of the active PGMs species depends on the type of metals and support materials as well as the reaction conditions, and hence, continuous efforts should be devoted to elucidate the effect of the oxidation state of PGMs on the catalytic activity. For this purpose, the oxidation state of PGMs should be conveniently and accurately estimated. Although XPS (X-ray photoelectron spectroscopy) has been the most commonly used method for this purpose, the XPS spectra of PGM catalysts containing the metal species of various oxidation states generally give a poorly resolved broad feature [11,12,16–18].

X-ray absorption spectroscopy (XAS) is a powerful method to characterize the electronic state of metal catalysts [19]. The white line feature at L_3-edge X-ray absorption near-edge structures (XANES) of transition metal compounds is typically assigned to electron transition from $2p_{3/2}$ to $5d_{3/2}$ and $5d_{5/2}$, and hence the area intensity of the white line can be an index for the oxidation state of the transition metals. Most of the L_3-edge XANES studies of heterogeneous catalysts have been focused on 5d transition metals, such as W [20], Re [21], Pt [1–10], and Au [22]. In contrast, less attempts have been focused on L_3-edge XAS studies of 4d (Pd [23–25], Ru [26], and Ag [27]) and 3d (Cu [28,29], Co [30,31], Fe [30]) transition metals-based catalysts. Previously, Chen et al. [32] reported a XANES study of the electronic structure of 4d transition metals

* Corresponding author. Tel.: +81 11 706 9240; fax: +81 11 706 9163.
E-mail address: kshimizu@cat.hokkai.ac.jp (K.-i. Shimizu).

0926-3373/$ – see front matter © 2011 Elsevier B.V. All rights reserved.
doi:10.1016/j.apcatb.2011.11.002

Table 1
Preparation conditions and structural information of the catalysts.

Catalysts	T_{CO} (K)[a]	t_{CO} (min)[b]	x[c]	D (nm)[d]	ΔE_K (eV)[e]	L_3 WL area intensity (a.u.)[f]
Rh_2O_3/SiO_2	–	–	3.0	–	4	29.4
$Rh_2O_{2.6}/SiO_2$	673	0.5	2.6	–	4	28.5
$Rh_2O_{1.9}/SiO_2$	673	1	1.9	6.8	2	18.1
$Rh_2O_{1.4}/SiO_2$	673	2	1.4	7.7	1	17.6
$Rh_2O_{0.6}/SiO_2$	973	60	0.6	11.5 (16.8)	0	8.2
Rh metal	–	–	0	–	0	5.1

[a] Temperatures of CO reduction treatment.
[b] Time of CO reduction treatment.
[c] Average oxidation number of the supported Rh species estimated from the amount of CO_2 formation during the CO reduction treatment.
[d] Average particle size of Rh metal from XRD analysis. The value in parenthesis is determined by CO adsorption method.
[e] Energy shift of the threshold of K-edge absorption from that for Rh metal powder as an indicator for Rh oxidation state. The threshold was defined as the point which intensity was 0.4 in the normalized XANES.
[f] White line area intensity at L_3-edge after subtraction of the continuum absorption.

(Mo, Tc, Ru, Pd, Ag) and showed that the white line area intensity of them increased linearly with increasing atomic number. The result illustrates the proportionality of the 4d-hole count to the white line area. Yoshida et al. [4] demonstrated a simple method to quantify Pt oxidation state in supported Pt catalysts using the white line area intensity at Pt L_3-edge XANES. They studied the oxidation state of Pt in various catalysts using two different techniques (the white line area intensity at Pt L_3 edge XANES and the area of O_2-TPD profile) and verified the quantitative correlation between the Pt oxidation state and the white line area intensity. Although Rh is an important element in catalysis, to the best of our knowledge, there are no Rh L_3-edge XANES studies on the structure-activity relationship of Rh catalysts. In the present study, we prepared a series of Rh/SiO_2 catalysts by controlling the average oxidation number (x) and recorded their Rh L_3-edge XANES spectra, followed by evaluation of the white line area intensity as an index of oxidation state. A linear relationship between the average Rh oxidation state and the white line intensity will verify that the quantitative determination of Rh oxidation state by the present simple XANES analysis. These catalysts were also characterized by various conventional methods (CO adsorption, X-ray diffraction, and Rh K-edge XAS) including the catalytic test, in order to demonstrate the advantages and utility of the present analysis using the Rh L_3-edge XANES.

2. Experimental

2.1. Catalyst preparation

SiO_2-supported Rh catalysts with Rh loading of 5 wt% were prepared by impregnating SiO_2 powder (Q-10, Fuji Silysia Chemical Ltd., 300 $m^2\,g^{-1}$) with an aqueous HNO_3 solution of $Rh(NO_3)_3$, followed by evaporation to dryness at 353 K, drying at 393 K for 12 h, and calcination in air at 973 K for 1 h. As shown below, Rh species existed as Rh_2O_3 in the as-calcined catalyst, referred to as Rh_2O_3/SiO_2. The oxidized sample (Rh_2O_3/SiO_2) was finally reduced in a flow of a CO/He gas mixture (0.4% CO) at a flow rate of 100 $cm^3\,min^{-1}$, and the gas formed during this CO-reduction treatment was continuously analyzed by non-dispersive infrared CO/CO_2 analyzers (Horiba VIA510). By changing the temperature (673 or 973 K) and time (0.5–60 min) of the CO-reduction treatment, a series of Rh_2O_x/SiO_2 catalysts with different average oxidation number of Rh (x) were prepared as summarized in Table 1.

2.2. Characterization

H_2-TPR of Rh_2O_3/SiO_2 was carried out using BELCAT (Bel Japan) in H_2 (5%)/Ar flow (30 $cm^3\,min^{-1}$) at a heating rate of 10 K min^{-1}. H_2 concentration was monitored with TCD, and water produced during the reduction process was removed by MS3A. The results showed a H_2 consumption peak in a temperature range from 360 K to 460 K. The H_2 consumption (0.727 mmol g^{-1}) was nearly consistent with the number of oxygen atoms in the supported Rh_2O_3 (0.729 mmol g^{-1}) in Rh_2O_3/SiO_2. This confirmed that the oxidation state of Rh(III) in the Rh_2O_3/SiO_2 sample.

X-ray diffraction (XRD) patterns of the powdered catalysts were recorded with a Rigaku MiniFlex II/AP diffractometer with Cu Kα radiation. Average metal particle size was calculated from the half-width of the diffraction at 41.1° in the XRD pattern using Scherrer equation. Only for the $Rh_2O_{0.6}/SiO_2$ sample pre-reduced in H_2 at 473 K, the number of surface metal atoms and the average particle size were estimated by the CO pulse adsorption method at 195 K [33] in a flow of He, on an assumption that CO was adsorbed on the surface of semi-spherical Rh particles at the CO/(surface Rh atom) ratio of 1/1.

Rh K-edge XAS measurement was carried out in a transmission mode with a Si(1 1 1) monochromator at BL14B2 of SPring-8 (Hyogo, Japan) operated at 8 GeV. The analyses of the extended X-ray absorption fine structure (EXAFS) and XANES were performed using the REX version 2.5 program (RIGAKU). The Fourier transformation of the k^3-weighted EXAFS from k space to R space was carried out over the k range 40–160 nm^{-1}. A part of the Fourier-transformed EXAFS in the R range of 1.1–3.0 Å were inversely Fourier-transformed, followed by the analysis with a usual curve fitting method in the k range of 40–160 nm^{-1} using empirical parameters for the phase shift and the amplitude functions for the Rh–Rh and Rh–O shells extracted from the data for Rh foil and Rh_2O_3, respectively.

Rh L_3-edge XANES spectra were obtained at BL-9A station of KEK-PF (Tsukuba, Japan) with a ring energy of 2.5 GeV and a stored current of 250–350 mA. The spectra were recorded in a transmission mode at room temperature with a Si(1 1 1) double-crystal monochromator. The background subtraction and normalization were performed by the REX version 2.5. The white line area intensity of normalized Rh L_3-edge XANES spectrum was evaluated by subtracting a function for the continuum absorption, Eq. (1):

$$a(E) = 0.5 + \pi^{-1}\ \tan^{-1}\left\{\frac{(E - E_0)}{\omega_0}\right\}, \quad (1)$$

From the normalized XANES spectrum [4], where E: X-ray energy (eV), $a(E)$: a function for the continuum absorption, ω_0: a width, E_0: an inflection point (eV). In the present simple calculation, ω_0 was fixed as 0.33 [4]. Although it should be related to the natural width of 2p electron and the experimental condition, it is noted that changes in the ω_0 value in a range of 0.2–0.5 resulted in negligible changes in the white line area intensity (±0.02%). The value of E_0 was assumed to be the same as the peak position of the white line.

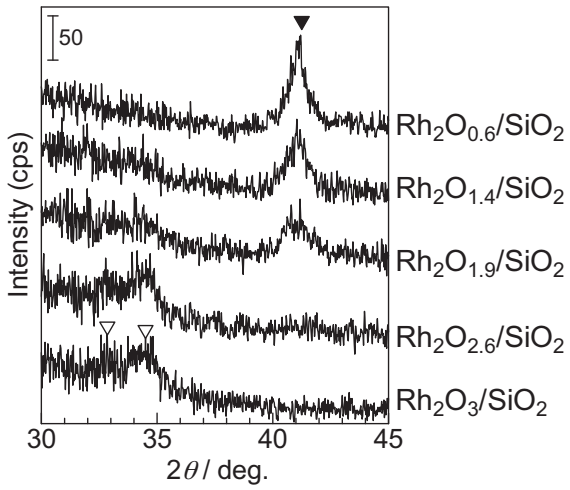

Fig. 1. XRD patterns of the Rh_2O_x/SiO_2 samples: (▽) Rh_2O_3, and (▼) Rh metal.

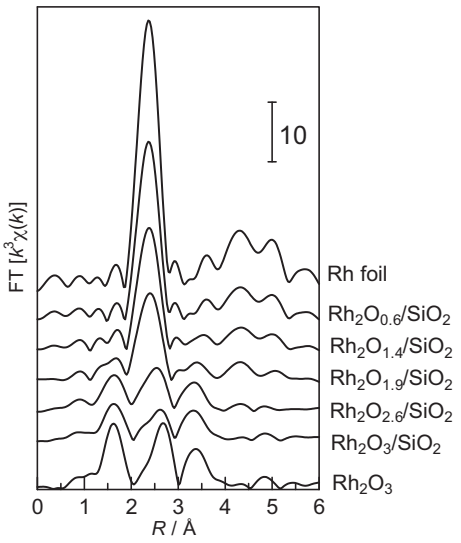

Fig. 2. Fourier transforms of Rh K-edge EXAFS for the samples and the reference compounds.

2.3. CO oxidation

Catalytic CO oxidation was performed in a fixed-bed flow reactor (inner diameter = 4 mm) at 373 K. A gas mixture of $CO/O_2/He$ (0.46%/10%/balance) was fed at a flow rate of 100 cm^3 min^{-1}. The effluent gas was analyzed by non-dispersive infrared CO/CO_2 analyzers (Horiba VIA510). Reaction rates per gram of the Rh_2O_x/SiO_2 catalysts for the CO oxidation were estimated at the reaction time (t) of 180 s under the condition where CO conversion was below 40% by changing the catalyst amount (40–70 mg). Note that time-conversion profiles of the CO oxidation showed that catalytic activity slightly changes with the reaction time. For example, CO conversion over $Rh_2O_{1.4}/SiO_2$ decreased from 31.9% to 29.2% when the reaction time increased from 180 s to 1800 s. However, in the initial period (t < 180 s), the activity did not markedly change (32.5% conversion at t = 0 s, where the gas in the reactor was completely changed from He to $CO + O_2$). So, it is reasonable to assume that at t = 180 s the oxidation state of supported Rh does not essentially different from that in an ambient condition where XAFS characterization is carried out.

3. Results and discussion

3.1. Conventional characterizations

Table 1 summarizes the structural information derived from various conventional experiments for characterization. The crystal phase was confirmed by XRD (Fig. 1). In the XRD pattern of the as-calcined sample, Rh_2O_3/SiO_2, lines due to Rh metal were absent, and broad lines assignable to Rh_2O_3 were observed. By changing the conditions for the CO reduction of the Rh_2O_3/SiO_2 sample, we prepared a series of the Rh_2O_x/SiO_2 samples with various oxidation states. The average oxidation number (x) was estimated from the amount of CO_2 molecules formed during the CO reduction treatment, according to the following stoichiometry: $(3-x)\ CO + Rh_2O_3 = (3-x)\ CO_2 + Rh_2O_x$. As expected, the oxidation number (x) decreased with increasing temperature and time of the CO reduction, accompanying a decrease in the diffraction intensity for the Rh_2O_3 phase and an increase in that for Rh metal. Although the catalysts after CO reduction at 973 K were not completely reduced (x = 0.6), the lines due to Rh_2O_3 were nearly absent in the XRD pattern of the $Rh_2O_{0.6}/SiO_2$ sample. The average size of the metallic Rh crystallites estimated using Scherrer equation (11.5 nm) was smaller than that estimated from the CO adsorption experiment (16.8 nm), implying the presence of Rh species inactive to CO adsorption. This result suggests that Rh species in the $Rh_2O_{0.6}/SiO_2$ sample are not fully reduced to metallic Rh. In summary, five kinds of the Rh_2O_x/SiO_2 catalysts with different average oxidation number were prepared as listed in Table 1.

Fig. 2 shows Fourier transforms of k^3-weighted Rh K-edge EXAFS. Peaks appearing at 1–2 Å are due to the adjacent oxygen atoms, and peaks at 2–3 Å is due to Rh atoms in metallic Rh or Rh_2O_3. The EXAFS curve fitting analysis provided the values of the coordination numbers and the distances for these Rh–O and Rh–Rh shells as listed in Table 2. The EXAFS of the $Rh_2O_{0.6}/SiO_2$ sample consisted of a Rh–Rh contribution with the coordination number of 7.1 and the bond distance of 2.69 Å. This Rh–Rh distance is identical to that of the metallic Rh (2.687 Å). Thus it is clear that metallic Rh is the predominant Rh species in the $Rh_2O_{0.6}/SiO_2$ sample, which is consistent with the result obtained from the XRD patterns. Considering the crystallographic data of Rh_2O_3 (Table 1), the EXAFS of the Rh_2O_3/SiO_2 sample in the R range of 1.1–3.0 Å (in Fig. 2) may be analyzed with three shells: a Rh–O shell at 2.04 Å and two Rh–Rh

Table 2
Results of curve-fitting analysis of Rh K-edge EXAFS.

Sample	Shell	N[a]	R (Å)[b]	σ (Å)[c]	R_f (%)[d]
Rh_2O_3/SiO_2	O	4.5	2.03	0.076	1.8
	Rh	0.9	2.78	0.039	
$Rh_2O_{2.6}/SiO_2$	O	4.4	2.04	0.076	2.3
	Rh	2.6	2.76	0.066	
$Rh_2O_{1.9}/SiO_2$	O	3.0	2.03	0.069	0.4
	Rh	5.4	2.70	0.069	
$Rh_2O_{1.4}/SiO_2$	O	1.8	2.07	0.059	1
	Rh	5.6	2.69	0.059	
$Rh_2O_{0.6}/SiO_2$	Rh	7.1	2.69	0.055	0.9
Rh_2O_3	O	(6.0)[e]	(2.04)[e]	–	–
	Rh	(1)[e]	(2.715)[e]	–	–
	Rh	(3)[e]	(2.988)[e]	–	–
Rh metal	Rh	(12)[f]	(2.689)[f]	–	–

[a] Coordination number.
[b] Interatomic distance.
[c] Debye–Waller factor.
[d] Residual factor.
[e] Crystallographic values for Rh_2O_3 [34].
[f] Crystallographic values for Rh metal [35].

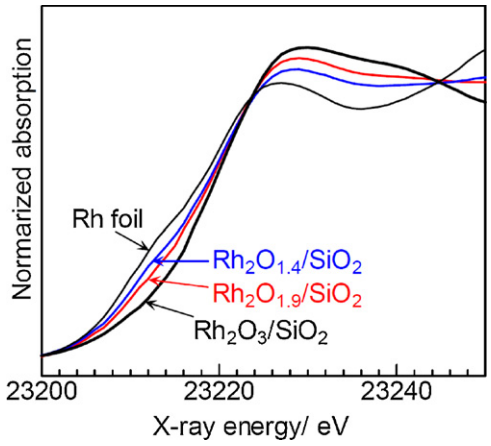

Fig. 3. Rh K-edge XANES spectra for the representative samples.

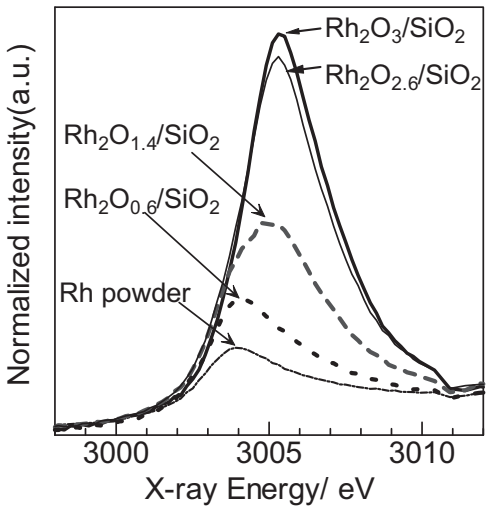

Fig. 4. Rh L_3-edge XANES spectra for the samples.

shells as the second and the third coordination spheres at 2.72 and 2.99 Å, respectively. However, the curve-fitting with two shells (a Rh–O shell at 2.03 Å and a Rh–Rh shell at 2.80 Å) gave a better fitting result than that with three shells, which might be due to an amorphous nature of the supported Rh_2O_3 species as suggested by the very broad diffraction lines for Rh_2O_3 (Fig. 1). The curve-fitting analysis of the Rh_2O_x/SiO_2 samples (x = 1.4, 1.9, 2.6) containing two phases (Rh metal and Rh_2O_3) was difficult, because the crystallographic Rh–Rh distances of Rh metal (2.689 Å) and Rh_2O_3 (2.715 Å) are close to each other. Actually, in our analytical conditions, the fitting with two shells (a Rh–O shell around 2.03–2.07 Å and a Rh–Rh shell around 2.69–2.76 Å) gave the best fit for these samples (Table 2). There are general tendencies that a decrease in the oxidation number (x) in the Rh_2O_x/SiO_2 samples results in a decrease in the coordination number for the Rh–O shell and an increase in the coordination number for the Rh–Rh shell. However, it is difficult to obtain a quantitative index of the oxidation state of the Rh species from these results because of some difficulties in the curve-fitting analyses as mentioned above.

Rh K-edge XANES spectra of some representative Rh_2O_x/SiO_2 samples are shown in Fig. 3. It is confirmed that the threshold energy shifts to higher energy as the oxidation number of X-ray absorbing atom is increased. In this study, the threshold was defined as the point which intensity was 0.4 in the normalized XANES spectra. This would be an indicator for the Rh oxidation state as listed in Table 1. As expected, there is a tendency that a decrease in the oxidation number (x) for the Rh_2O_x/SiO_2 samples results in a decrease in the threshold energy. However, catalysts with different oxidation number (the $Rh_2O_{2.6}/SiO_2$ and Rh_2O_3/SiO_2 samples) gave the same threshold energy within the experimental error. In addition, the XANES spectrum of the $Rh_2O_{0.6}/SiO_2$ sample (not shown) was nearly identical to that of the Rh powder in a range of 23.20–23.22 keV. From the above discussion, it can be concluded that XRD and K-edge XANES/EXAFS are not useful in the quantitative determination of the average oxidation state of the Rh_2O_x/SiO_2 catalysts.

3.2. Quantification of Rh oxidation state by L_3-edge XANES analysis

Fig. 4 shows Rh L_3-edge absorption spectra of the Rh_2O_x/SiO_2 samples and Rh powder. As previously reported by Chen et al. [32], the XANES spectrum of Rh powder, a reference compound of metallic Rh, showed a small white line due to lack of 4d-hole. In contrast, the XANES spectrum of the Rh_2O_3/SiO_2 sample exhibited a large white line peak centered at 3005.3 eV with an almost symmetric shape. This peak should be predominantly assignable to the electron transition from $2p_{3/2}$ to $5d_{3/2}$ and $5d_{5/2}$, and hence, it is expected that the area intensity of the white line can become an index for the oxidation state of Rh species. As the average oxidation number of the Rh_2O_x/SiO_2 samples increased, the area intensity of the white line increased, indicating an increase of vacancy in the d-states. Modifying the method by Yoshida et al. [4] for the Pt L_3-edge XANES analysis, the area intensity of the white line was determined as illustrated in Fig. 5. An arctangent function shown as a dashed line, which corresponds the continuum absorption, is subtracted from the raw spectrum (dots) to give a band corresponding to an absorption predominantly related to the electron transition from $2p_{3/2}$ to $5d_{3/2}$ and $5d_{5/2}$ (solid line). The white line area intensities thus estimated were listed in Table 1, and also plotted as a function of the average oxidation number of the Rh_2O_x/SiO_2 samples and Rh powder as shown in Fig. 6. It is noted that the white line area intensity increased linearly with increasing the oxidation number. This clearly indicates that the white line area intensity at the Rh L_3-edge XANES is a quantitative index of the Rh oxidation state. Therefore, it is concluded that the present method of Rh L_3-edge XANES analysis can be used for the quantitative estimation of the average oxidation

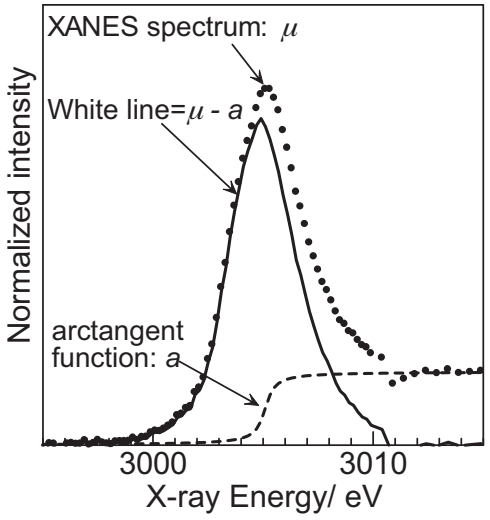

Fig. 5. An example for the simple method for Rh L_3-edge XANES analysis. The spectrum was for the $Rh_2O_{1.9}/SiO_2$ sample. An arctangent function (broken line) for the continuum absorption is subtracted from the raw spectrum (dots) to give a band corresponding to the white line peak (solid line).

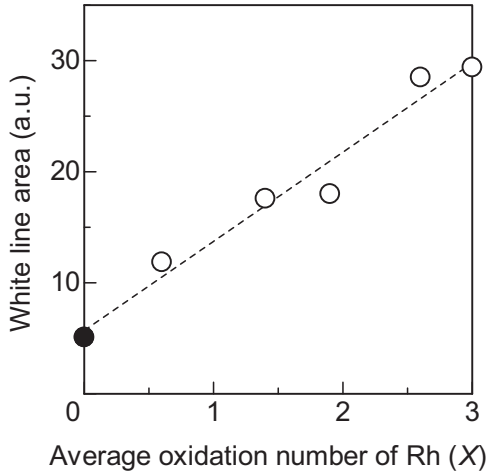

Fig. 6. Relation between the average oxidation number (x) and the white line area intensity of the Rh L_3-edge XANES of (○) the Rh_2O_x/SiO_2 samples and (●) Rh powder.

number of structurally unknown Rh samples. Taking into account the fact that XPS spectra of Rh samples containing Rh species of different oxidation states give a poorly resolved broad feature [16–18], this method would be widely acceptable as a novel characterization method for a quantification of the Rh oxidation states in various Rh compounds.

3.3. Structure–activity relationship

Finally, in order to demonstrate a utility of this method in a catalytic study, the effect of the average Rh oxidation number (x) on the catalytic activity of the Rh_2O_x/SiO_2 samples for CO oxidation was examined. The rates of CO oxidation with molecular oxygen to produce CO_2 over these samples were measured at 373 K. As shown in Fig. 7, the rates per gram of the catalyst increased with a decrease in the average oxidation number up to 1.4 and then decreased with further decease in the oxidation number. One may consider that this result might be an indication of partially oxidized Rh particles (such as Rh metal particles with surface oxide layers) as the most active species. However, if the turnover frequency (TOF) per surface Rh metal atom for the $Rh_2O_{0.6}/SiO_2$ and $Rh_2O_{1.4}/SiO_2$ samples were tentatively calculated from the average particle size of the metallic Rh in the $Rh_2O_{0.6}/SiO_2$ and $Rh_2O_{1.4}/SiO_2$ samples, i.e., 11.5 nm and 7.7 nm, respectively (Table 1), they were 0.020 s^{-1} and 0.019 s^{-1}, respectively, suggesting that the lower activity of the $Rh_2O_{0.6}/SiO_2$ catalyst than that of the $Rh_2O_{1.4}/SiO_2$ catalyst should be simply due to the larger particle size. On the other hand, the results for the rest of the samples clearly exhibited that the catalytic activity decreased with increasing the average Rh oxidation number (x), i.e., with decreasing the number of the active Rh^0 sites. Thus, it is suggested that the Rh^0 sites in the Rh_2O_x/SiO_2 samples would be the catalytic active sites for CO oxidation under the present reaction condition, though further examinations may be required to obtain a conclusive model of active species.

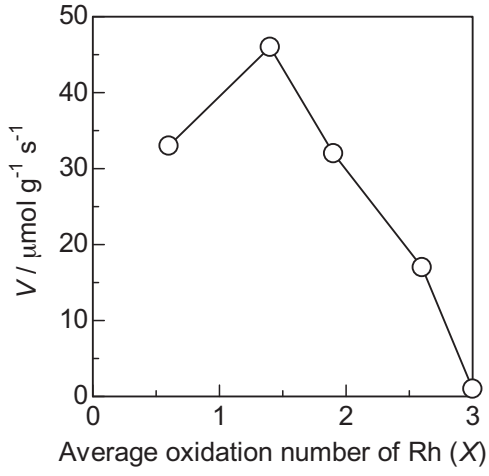

Fig. 7. Effect of the average oxidation number (x) on the reaction rate (V) for CO oxidation at 373 K over the Rh_2O_x/SiO_2 catalysts. Reaction conditions: 0.4% CO, 10% O_2.

The above discussion was based on the accurate oxidation number of the Rh species, which was determined by the chemical method recorded during the catalyst preparation and also confirmed by the spectroscopic method recorded after the catalyst preparation. However, for the samples that are not applicable with the chemical method, such as Rh catalyst supported by highly reducible supports and Rh catalysts with transition metal additives, the spectroscopic method will be the only way to determine the accurate oxidation number. In this study, we presented a simple L_3-edge XANES analysis for the quantitative estimation of the average oxidation number of Rh species. It is claimed that, hereafter, this method will be available to discuss the effect of Rh oxidation state on the activity of Rh catalysts, even when the determination of the Rh oxidation state is difficult by other characterization methods.

4. Conclusion

A simple method of Rh L_3-edge XANES analysis is presented to quantify the oxidation states of Rh species in a series of supported Rh catalysts containing different amount of Rh metal and Rh_2O_3 phases. The linear relationship between the average oxidation numbers determined by a chemical method (the number of CO_2 formed during pre-reduction by CO) and the white line intensities at the Rh L_3-edge XANES verifies that this method is effective for a quantification of the average Rh oxidation number in structurally unknown Rh samples. Especially, this method will be powerful tool when the chemical method is not available.

Acknowledgments

The XAS measurements at Spring-8 were conducted with the approval of the Japan Synchrotron Radiation Research Institute (JASRI) (Proposal No. 2008B2066). The XAS measurements at KEK-PF were performed under the approval of the Photon Factory Program Advisory Committee (No. 2008G024). This work was supported by the Japanese Ministry of Education, Culture, Sports, Science and Technology via Grant-in-Aids for Scientific Research B (23360354) and for Young Scientists A (22686075).

References

[1] H. Yoshitake, Y. Iwasawa, J. Phys. Chem. 96 (1992) 1329–1334.
[2] Y. Yazawa, N. Takagi, H. Yoshida, S. Komai, A. Satsuma, T. Hattori, Appl. Catal. A 233 (2002) 103–112.
[3] Y. Yazawa, H. Yoshida, S. Komai, T. Hattori, Appl. Catal. A 233 (2002) 113–124.
[4] H. Yoshida, S. Nonoyama, Y. Yazawa, T. Hattori, Phys. Scripta T115 (2005) 813–815.
[5] A.Y. Stakheev, Y. Zhang, A.V. Ivanov, G.N. Baeva, D.E. Ramaker, D.C. Koningsberger, J. Phys. Chem. C 111 (2007) 3938–3948.
[6] T. Tanabe, Y. Nagai, K. Dohmae, H. Sobukawa, H. Shinjoh, J. Catal. 257 (2008) 117–124.
[7] J. Singh, E.M.C. Alayon, M. Tromp, O.V. Sofanova, P. Glatzel, M. Nachtegaal, R. Frahm, J.A. van Bokhoven, Angew. Chem. Int. Ed. 47 (2008) 9260–9263.
[8] E. Becker, P.-A. Carlsson, H. Grönbeck, M. Skoglundh, J. Catal. 252 (2007) 11–17.
[9] J.-D. Grunwaldt, M. Beier, B. Kimmerle, A. Baiker, M. Nachtegaal, B. Griesebock, D. Lützenkirchen-Hecht, J. Stötzel, R. Frahm, Phys. Chem. Chem. Phys. 11 (2009) 8779–8789.
[10] K. Paredis, L.K. Ono, S. Mostafa, L. Li, Z. Zhang, J.C. Yang, L. Barrio, A.I. Frenkel, B.R. Cuenya, J. Am. Chem. Soc. 133 (2011) 6728–6735.

[11] Y. Yazawa, H. Yoshida, S. Komai, A. Satsuma, T. Hattori, Appl. Catal. B 19 (1998) 261–266.
[12] Y. Yazawa, H. Yoshida, N. Takagi, S. Komai, A. Satsuma, T. Hattori, J. Catal. 187 (1999) 15–23.
[13] S. Hinokuma, H. Fujii, M. Okamoto, K. Ikeue, M. Machida, Chem. Mater. 22 (2010) 6183–6190.
[14] J.-D. Grunwaldt, L. Basini, B.S. Clausen, J. Catal. 200 (2001) 321–329.
[15] K. Dohmae, Y. Nagai, T. Tanabe, A. Suzuki, Y. Inada, M. Nomura, Surf. Interface Anal. 40 (2008) 1751–1754.
[16] K. Dohmae, T. Nonaka, Y. Seno, Surf. Interface Anal. 37 (2005) 112–119.
[17] M. Zimowska, J.B. Wagner, J. Dziedzic, J. Camra, B. Borzecka-Prokop, M. Najbar, Chem. Phys. Lett. 417 (2006) 137–142.
[18] M.E. Grass, Y. Zhang, D.R. Butcher, J.Y. Park, Y. Li, H. Bluhm, K.M. Bratlie, T. Zhang, G.A. Somorjai, Angew. Chem. Int. Ed. 47 (2008) 8893–8896.
[19] S.R. Bare, T. Ressler, Adv. Catal. 52 (2009) 339–465.
[20] S. Yamazoe, Y. Hitomi, T. Shishido, T. Tanaka, J. Phys. Chem. C 112 (2008) 6869–6879.
[21] S.R. Bare, S.D. Kelly, F.D. Vila, E. Boldingh, E. Karapetrova, J. Kas, G.E. Mickelson, F.S. Modica, N. Yang, J.J. Rehr, J. Phys. Chem. C 115 (2011) 5740–5755.
[22] C.K. Costello, J. Guzman, J.H. Yang, Y.M. Wang, M.C. Kung, B.C. Gates, H.H. Kung, J. Phys. Chem. B 108 (2004) 12529–12536.
[23] I. Davoli, S. Stizza, A. Bianconi, M. Benfatto, C. Furlani, V. Sessa, Solid State Commun. 48 (1983) 475–478.
[24] T. Kubota, Y. Kitajima, K. Asakura, Y. Iwasawa, Bull. Chem. Soc. Jpn. 72 (1999) 673–681.
[25] M.W. Tew, J.T. Miller, J.A. van Bokhoven, J. Phys. Chem. C 113 (2009) 15140–15147.
[26] J.G. Zhou, H.T. Fang, Y.F. Hu, T.K. Sham, C.X. Wu, M. Liu, F. Li, J. Phys. Chem. C 113 (2009) 10747–10750.
[27] T. Miyamoto, H. Niimi, Y. Kitajima, T. Naito, K. Asakura, J. Phys. Chem. A 114 (2010) 4093–4098.
[28] K. Shimizu, H. Maeshima, H. Yoshida, A. Satsuma, T. Hattori, Phys. Chem. Chem. Phys. 2 (2000) 2435–2439.
[29] K. Shimizu, H. Maeshima, H. Yoshida, A. Satsuma, T. Hattori, Phys. Chem. Chem. Phys. 3 (2001) 862–866.
[30] D. Bazin, L. Guczi, Appl. Catal. A 231 (2001) 147–162.
[31] F. Zheng, S. Alayoglu, J. Guo, V. Pushkarev, Y. Li, P.-A. Glans, J. Chen, G. Somorjai, Nano Lett. 11 (2011) 847–853.
[32] J. Chen, E. Kemly, M. Croft, Y. Jcon, X. Xu, S.A. Shaheen, P.H. Ansari, Solid State Commun. 85 (1993) 291–296.
[33] T. Tanabe, Y. Nagai, T. Hirabayashi, N. Takagi, K. Dohmae, N. Takahashi, S. Matsumoto, H. Shinjoh, J.N. Kondo, J.C. Schouten, H.H. Brongersma, Appl. Catal. A 370 (2009) 108–113.
[34] J.M.D. Coey, Acta Cryst. B26 (1970) 1876–1877.
[35] H.P. Singha, Acta Cryst. A24 (1968) 469–471.